Experimental and theoretical investigation of the reaction $NH(X\,^3\Sigma^-)+H(^2S)\rightarrow N(^4S)+H_2(X\,^1\Sigma_g^+)$

L. Adam and W. Hack
Max-Planck-Institut für biophysikalische Chemie, D-37077 Göttingen, Germany

H. Zhu, Z.-W. Qu, and R. Schinke[a)]
Max-Planck-Institut für Dynamik und Selbstorganisation, D-37073 Göttingen, Germany

(Received 20 December 2004; accepted 6 January 2005; published online 16 March 2005)

The rate coefficient of the reaction $NH(X\,^3\Sigma^-)+H(^2S)\xrightarrow{k_{1a}}N(^4S)+H_2(X\,^1\Sigma_g^+)$ is determined in a quasistatic laser-flash photolysis, laser-induced fluorescence system at low pressures (2 mbar$\leqslant p \leqslant$10 mbar). The NH(X) radicals are produced via the quenching of NH($a^1\Delta$) (obtained by photolyzing HN_3) with Xe whereas the H atoms are generated in a H_2/He microwave discharge. The NH(X) concentration profile is measured under pseudo-first-order condition, i.e., in the presence of a large excess of H atoms. The room temperature rate coefficient is determined to be $k_{1a}=(1.9\pm0.5)\times10^{12}$ cm^3 mol^{-1} s^{-1}. It is found to be independent of the pressure in the range considered in the present experiment. A global potential energy surface for the $^4A''$ state is calculated with the internally contracted multireference configuration interaction method and the augmented correlation consistent polarized valence quadruple zeta atomic basis. The title reaction is investigated by classical trajectory calculations on this surface. The theoretical room temperature rate coefficient is $k_{1a}=0.92\times10^{12}$cm^3 mol^{-1} s^{-1}. Using the thermodynamical data for the atoms and molecules involved, the rate coefficient for the reverse reaction, k_{-1a}, is also calculated. At high temperatures it agrees well with the measured k_{-1a}. © *2005 American Institute of Physics*.
[DOI: 10.1063/1.1862615]

I. INTRODUCTION

The NH_i ($i=1,2$) radicals are of essential importance for understanding the nitrogen chemistry in flames[1,2] as well as the De–NO_x and RAPRENO$_x$ (rapid reduction of NO_x) combustion processes. The simplest reaction among these is

$$NH(X\,^3\Sigma^-)+H(^2S)\xrightarrow{k_1}\text{products}. \tag{1}$$

The possible products are $N(^4S)+H_2$ and NH_2 (see Fig. 1).

Reaction (1) has been studied at high temperatures in the range 1790 K$\leqslant T\leqslant$2200 K in rich premixed $H_2/O_2/Ar$ flames doped with CH_3CN.[3] The NH(X) concentration has been followed by laser-induced fluorescence (LIF). The rate of removal of NH(X) has been found to depend linearly on the H atom concentration for a range of stoichiometries, indicating that NH(X) is mainly removed by reaction (1). From the proportionality and an approximate calibration for NH(X) a rate coefficient $k_1(1790\text{ K})=3\times10^{13}$ cm^3 mol^{-1} s^{-1} has been obtained, which has been assumed to be accurate within a factor of 2. The reaction rate coefficient $k_1(T)$ has been found to increase with increasing temperature, i.e., for $T=2200$ K a value $k_1(2200\text{ K})=4.7\times10^{13}$ cm^3 mol^{-1} s^{-1} has been determined. Up to now, the rate coefficient for reaction (1) has not yet been measured at low temperatures directly. On the other hand, the decomposition $NH_2(\tilde{X})\rightarrow NH(X)+H(^2S)$ as well as the reverse reaction $N(^4S)+H_2(X\,^1\Sigma_g^+)\rightarrow NH(X)+H(^2S)$ have been examined.[4–8]

There are three recent theoretical investigations of the reaction

$$NH(X\,^3\Sigma^-)+H(^2S)\xrightarrow{k_{1a}}N(^4S)+H_2(X\,^1\Sigma_g^+), \tag{1a}$$

which is one of the possible pathways of reaction (1) and the focus of this study. It proceeds on the potential energy sur-

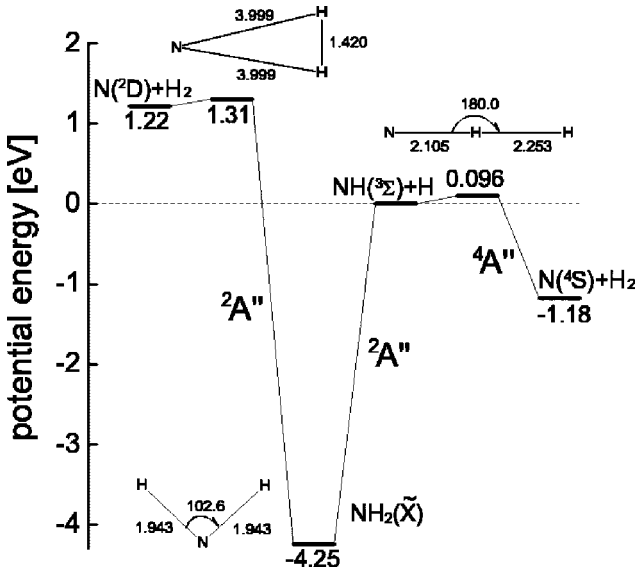

FIG. 1. Schematic energy level and correlation diagram for the reaction $NH(X\,^3\Sigma^-)+H(^2S)\rightarrow$products. The energies and transition state geometries are the ones calculated in this work (avqz atomic basis).

a)Electronic mail: rschink@gwdg.de

face (PES) of the $^4A''$ ($^4\Sigma^-$ in linear N–H–H configuration) electronic state (Fig. 1). Xu *et al.*[9] and Zhang and Truong[10] used several versions of transition state theory (TST) to determine the rate coefficient $k_{1a}(T)$ over a large temperature range. The geometry of the transition state (TS), the energy at the TS, as well as the TS frequencies of the $^4A''$ PES, required in the TST approach, were obtained by *ab initio* electronic structure calculations on various levels of theory. Pascual *et al.*[11] used classical trajectories to investigate reaction (1a) on a global $^4A''$ PES obtained from *ab initio* electronic structure calculations. This PES was constructed by Sheppard interpolation from a very small number of geometries. The three theoretical rate coefficients k_{1a} agree very well with each other at high temperatures ($T \approx 2000$ K), but strongly deviate at room temperature; the deviation at 300 K between the lowest[11] and the highest[9] rate coefficient is more than an order of magnitude.

Within the experimental uncertainty, the three theoretical rate coefficients k_{1a} agree with the rate coefficient k_1 of Morley[3] for reaction (1). The rate coefficients k_1 and k_{1a} can be compared for the following reasons. According to the correlation diagram in Fig. 1 (see also Fig. 1 of Takayanagi *et al.*, Ref. 12) $NH(X\,^3\Sigma^-) + H(^2S)$ correlates with both states of NH_2, i.e., the $^2A''$ state and the $^4A''$ state. The first state correlates with the electronic ground state of NH_2, whereas the PES of the latter state correlates with $N(^4S) + H_2(^1\Sigma_g^+)$. It is—except for a small barrier in the entrance channel—purely downhill. H atom exchange reactions proceeding on the $^2A''$ PES do not remove $NH(X)$. On the other hand, the $N(^2D) + H_2(X\,^1\Sigma_g^+)$ product channel is about 1.2 eV higher in energy than the reactant channel and therefore unaccessible even at high temperatures. Spin-forbidden transitions from the $^2A''$ to the $^4A''$ state are unlikely for reasons to be discussed below. Furthermore, the stabilization of $NH_2(\tilde{X})^{\ddagger}$ in collisions with bath atoms and molecules is negligible for the pressures employed in the present study. Thus, the removal of $NH(X)$ in collisions with H atoms can only occur via reactions on the $^4A''$ PES yielding the products $N(^4S)$ and $H_2(X\,^1\Sigma_g^+)$.

In this work we present a direct measurement of the rate coefficient of reaction (1) at room temperature (Sec. II), calculate a PES for the $^4A''$ state, and describe classical trajectory calculations for reaction (1a) on it (Sec. III). The experimental and theoretical results are compared and discussed in Sec. IV.

II. EXPERIMENT

A. Setup

The experiment is performed in a quasistatic laser-flash photolysis/LIF system, where "quasistatic" means that the flow through the reaction cell is negligible between the pump and the probe pulses, but sufficient to exchange the gas volume between two subsequent pump pulses (see below). The carrier gas is He at a total pressure in the range of $2.1\ \text{mbar} \leqslant p \leqslant 10.4\ \text{mbar}$.

The experimental setup is described in detail elsewhere,[13] and only the essentials are repeated here. For the photolysis a XeCl-exciplex laser (Lambda Physik LPX 205) with pulse energies in the range 200–400 mJ and a beam area of about 1.1 cm^2 is used. The probe laser is a dye laser (Lambda Physik FL 3002) with a beam area of 7 mm^2. It is pumped by an exciplex laser (Lambda Physik LPX 205, XeCl; 230–290 mJ).

The $NH(X)$ radicals are obtained by quenching $NH(a\,^1\Delta)$ with Xe; the $NH(a)$ radicals are produced by HN_3 photolysis in the $\tilde{A}$-$\tilde{X}$ band at $\lambda = 308$ nm. The H atoms are generated in a side arm of the reactor in a microwave discharge of a H_2/He mixture (5% molfraction H_2 in He). The absolute initial H atom concentration is determined via titration with NO_2. The increase of OH with increasing NO_2 is observed by LIF. The OH is observed via the $Q_1(2)$ line of the transition $A\,^2\Sigma^+, v=0 \leftarrow X\,^2\Pi, v=0$ at $\lambda = 308.01$ nm with a dye laser (Lambda Physik LPD 3002) pumped by a Nd:YAG (YAG—yttrium aluminum garnet) laser (Spectra Physics GC-R-3-10). $NH(X, v=0)$ is detected by exciting the $P_2(2)$ line at $\lambda = 336.48$ nm of the transition $A\,^3\Pi, v'=0 \leftarrow X\,^3\Sigma, v''=0$. The undispersed fluorescence from the excited state is observed in the wavelength range 335–337 nm perpendicular to the laser beam using a long pass filter (KV370, Schott) or an interference filter 336.3 nm (Schott) to suppress scattered radiation from the excitation beam.

The HN_3 and Xe are added to the reactor via an inner probe which ends 1 cm above the photolysis volume. The NO_2 for the titration is also added to the system through this probe. To improve the mixing a second He flow is added in both cases (HN_3/Xe or NO_2). The distance between the entrance of HN_3 and the photolysis volume is kept as small as possible to minimize the dark reaction of H atoms with HN_3 (see below). A distance of about 1 cm is found to be optimum for mixing on one side and limiting the dark reaction on the other.

Gases with the highest commercially available purity are used: He, 99.9999%, Praxair; Xe, 99.998%, Messer-Griesheim; N_2, 99.995%, UCAR; H_2, 99.999%, Praxair; and NO_2, 99.5%, Merck. HN_3 is synthesized by melting stearic acid, $CH_3(CH_2)_{16}COOH$ (97%, Merck), with NaN_3 (99.0%, Merck). It is dried with $CaCl_2$ and stored in a bulb at partial pressures $\leqslant 200$ mbar diluted with He (overall pressure ca. 1 bar). For safety reasons, the HN_3 containing devices are covered with a wooden box since HN_3 is highly explosive even at low pressures.

B. Results

The $NH(X)$ radicals are produced in the fast quenching reaction

$$NH(a\,^1\Delta) + Xe \xrightarrow{k_q} NH(X\,^3\Sigma^-) + Xe, \tag{2}$$

for which a rate coefficient $k_q = 5.8 \times 10^{12}\ \text{cm}^3\,\text{mol}^{-1}\,\text{s}^{-1}$ has been determined.[13] Typical $NH(X)$ concentration profiles in the absence and in the presence of H atoms are shown in Fig. 2. $NH(a)$ is formed at $t=0$ by the photolysis pulse. In both cases (with or without H atoms present), the $NH(X)$ concentration increases very rapidly in time due to the quenching of $NH(a)$ by Xe. In the absence of H atoms (discharge off, open circles in Fig. 2) the $NH(X)$ concentration stays constant after about $t = 50\ \mu$s for more than 300 μs. This means that

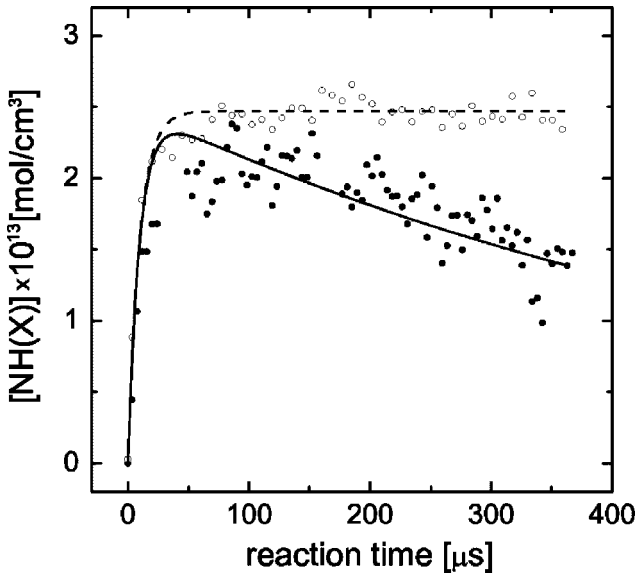

FIG. 2. NH(X) concentration profiles in the absence (○) and presence (●) of H atoms. The experimental conditions are those of experiment 11 in Table I. The lines have been determined as described in the text.

neither diffusion nor the other gases present in the system (H_2, HN_3) contribute to the NH(X) consumption (as expected from the rates and concentrations of these molecules). For the individual experiments the Xe concentration is in the range 1.3×10^{-8} mol cm$^{-3}\leqslant$[Xe]$\leqslant 1.8\times10^{-8}$ mol cm^{-3} as given in Table I. Thus, the NH(a) is depleted to about 1% in the time range 30–50 μs. The dashed line in Fig. 2 is obtained from a very simple simulation of the system assuming an initial NH(a) concentration of $[NH(a)]_0=2.6\times10^{-13}$ mol cm^{-3} estimated from the HN_3 absorption at the photolysis wavelength and a dissociation quantum yield of about 1. The subsequent analysis of the NH(X) profiles to determine k_{1a} start at about $t>50$ μs for all experimental conditions.

When H atoms are present, the experiment is complicated by a background concentration of NH(X), which is independent of time. It is due to the reaction of H atoms with the precursor molecule HN_3 according to

TABLE I. Experimental data for the 14 independent experiments.

p(mbar)	[Xe]×10^8 (mol/cm^3)	[HN_3]×10^{11} (mol/cm^3)	[H]×10^{10} (mol/cm^3)	k_{eff} (s^{-1})	$k_1\times10^{-12}$ (cm^3/mol s)
2.1	1.3	2.0	3.5	910	2.6
2.1	1.7	4.6	4.6	980	2.1
8.0	1.8	6.5	4.9	720	1.5
9.9	1.7	8.0	5.8	1170	2.0
10.0	1.7	6.5	4.8	950	2.0
10.0	1.7	8.0	4.7	550	1.2
10.1	1.7	8.0	4.8	920	1.9
10.1	1.7	6.8	3.1	790	2.5
10.1	1.7	8.0	4.7	460	1.0
10.1	1.7	7.4	4.7	1120	2.4
10.1	1.7	8.0	7.1	1630	2.3
10.2	1.3	3.4	4.7	480	1.0
10.2	1.7	8.0	2.4	340	1.4
10.4	1.0	5.0	3.6	940	2.6

$$2H + HN_3 \rightarrow H_2 + NH(X) + N_2. \quad (3)$$

In order to minimize this background the distance between the end of the HN_3 admixing probe and the laser photolysis volume, i.e., the time in which reaction (3) can occur, is kept as short as possible. It is limited, however, by the time required to mix HN_3 to the system, because it is necessary that a homogeneous mixture is photolyzed. Thus, a NH(X) background, $[NH(X)]_\infty$, independent of the reaction time (i.e., the time between photolysis and analysis pulse) is unavoidable and has to be subtracted from the signal. The (dark) NH(X) concentration $[NH(X)]_\infty$ is determined during the entire experiment.

The NH(X) concentration profile in Fig. 2 in the presence of H atoms shows a depletion which is due to reaction (1a). The H atom concentration is large compared to $[NH(X)]_0$ [i.e., the NH(X) concentration at a time >50 μs] and thus pseudo-first-order conditions are realized. From the slope of ln[NH(X)] versus time first-order rate coefficients k_{eff} are determined by

$$d\ln[NH(X)]/dt = k_{\text{eff}}[H]. \quad (4)$$

This k_{eff} is converted with the H atom concentrations into second-order rate coefficients k_{1a}.

The results for the 14 independent experiments are summarized in Table I. It is not possible to vary the H atom concentration over a wide range and therefore the dependence of the first-order rate coefficient versus [H] cannot be investigated. The rate measurements are performed mainly at two pressures around 2 and 10 mbar. Within the experimental uncertainty the same rate coefficients are obtained at both pressures. The final rate coefficient, obtained as the average of the 14 measurements summarized in Table I, is $k_1(298\ \text{K})=(1.9\pm0.5)\times10^{12}$ cm^3 mol^{-1} s^{-1}. The large uncertainty is mainly due to the titration of the H atoms and the scatter in the first-order rate coefficient. Since the rate is determined from the NH(X) depletion, only reaction (1a) contributes to k_1 and thus it can be stated $k_1=k_{1a}$ (see also the Discussion). With the thermodynamical data of Ref. 14 the exothermicity of reaction (1a) is calculated to be[15] $\Delta_R H=23.1$ kcal/mol. The room temperature rate coefficient for the reverse reaction, k_{-1a}, is estimated from the thermodynamical data and the measured rate coefficient k_{1a} to be of the order of only 10^{-5} cm^3 mol^{-1} s^{-1} (see also Sec. IV).

III. THEORY

A. Electronic structure calculations and potential energy surface

The electronic structure calculations for the $^4A''$ state of NH_2 are performed with the internally contracted multireference configuration interaction (MRCI) method.[16,17] In order to approximately account for higher excitations and size consistency the Davidson correction is applied.[18] The MRCI calculations are based on optimized full-valence complete-active space self-consistent field (CASSCF) orbitals.[19,20] If not stated otherwise, the augmented correlation consistent polarized valence quadruple zeta (aug-cc-pvqz) atomic basis set of Dunning[21] is employed. The 1s orbital of nitrogen is

TABLE II. Equilibrium bond distances (in a_0) and energy difference between reactants and products (in kcal/mol) for several basis sets.

Basis	$NH(X\,^3\Sigma^-)$	$H_2(X\,^1\Sigma_g^+)$	ΔE
avtz	1.967	1.404	28.07
avqz	1.963	1.402	27.25
av5z	1.961	1.401	27.04
av6z	1.961	1.401	26.95
Expt.	1.958[a]	1.401[a]	24.7[b]

[a]Reference 14.
[b]See discussion in the text.

fully optimized in the CASSCF calculations but frozen in the subsequent configuration interaction (CI) calculations. There are 35 reference configurations with 50 reference configuration state functions for the $^4A''$ state leading to 264 611 contracted configurations in the CI calculations. All calculations are performed in C_s symmetry using the MOLPRO suit of programs.[22]

First, we calculated the equilibrium geometries and energies of the reactants and products using several atomic basis sets; the results are summarized in Table II. The convergence is monotonic and the agreement with the experimental[14] equilibrium bond distances is excellent. The reaction energies (in kcal/mol) calculated in the previous *ab initio* studies are markedly higher than our value of about 27: 30.23, Xu *et al.*;[9] 29.16, Zhang and Truong;[10] and 30.1, Pascual *et al.*[11] Using the thermodynamical data[14,15] and a difference of the zero-point energies for NH and H_2 of 1.60 kcal/mol the corresponding experimental value is 24.7 kcal/mol.

The $^4A''$ PES has a small barrier at linearity in the NH + H reactant channel. This barrier governs the energy dependence of the reaction cross sections and therefore the rate coefficient for the exchange reaction. The bond distances and the barrier height as functions of the basis size are summarized in Table III. The barrier energy increases with increasing basis size. The values of the three previous calculations are similar (in kcal/mol): 1.88, Xu *et al.*;[9] 2.17, Zhang and Truong;[10] and 2.4, Pascual *et al.*[11]

The global three-dimensional PES of the $^4A''$ state is calculated employing the aug-cc-pvqz basis set; this is a reasonable compromise between accuracy and computational costs. With this basis set the entrance channel barrier is slightly underestimated by about 0.12 kcal/mol (corresponding to an energy of 60 K) as compared to the aug-cc-pv6z basis set. Because the exchange reaction is strongly favored in the near-linear NH–H approach, we use the following bond coordinates for constructing the PES: R_{NH}, R_{HH}, and α,

TABLE III. Bond distances (in a_0) and barrier energy (in kcal/mol) at the saddle point for several basis sets.

Basis	N–H[a]	H–H	Energy
avtz	2.099	2.289	1.906
avqz	2.105	2.253	2.202
av5z	2.109	2.238	2.290
av6z	2.110	2.234	2.323

[a]Bond angle $\alpha = 180°$.

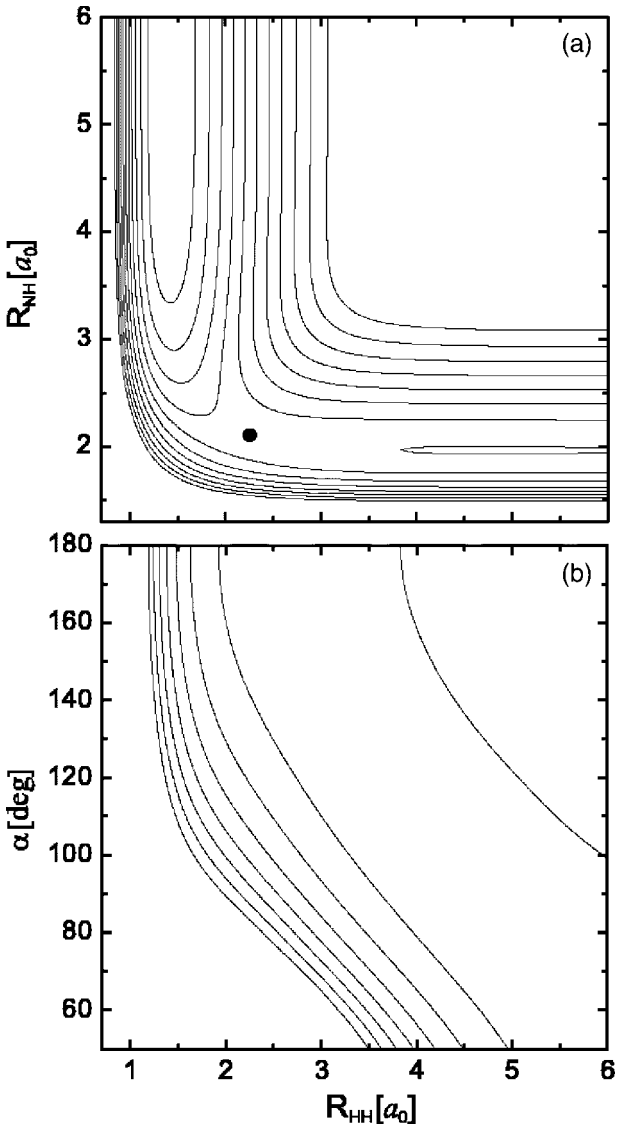

FIG. 3. (a) Contour plot of the $^4A''$ PES for the linear arrangement ($\alpha = 180°$). The highest contour is for an energy of 2.1 eV (measured with respect to the NH+H equilibrium) and the step size is 0.3 eV. The filled circle indicates the transition state. (b) Contour plot for fixed NH bond length $1.963a_0$. The other details are the same as in (a).

where α is the N–H–H angle. The N–H and H–H bond lengths (in a_0) are varied between 1.3–2.4, 2.4–3.4, 3.4–4.0, 4.0–5.0, and 5.0–8.0 with step sizes of 0.1, 0.2, 0.3, 0.5, and 1.0, respectively. For the H–H bond additional points between 0.5–1.3 with a step size of 0.1 have been included to the grid. The bond angle α (in degrees) is varied between 0–40 and 40–180 with step sizes of 5 and 10, respectively. In order to have a better representation at small angles, $\alpha = 2°$ is added to the angular grid. Altogether, $24 \times 32 \times 24 = 18\,432$ geometries have been considered. Interpolation between the grid points is done by a three-dimensional (3D) cubic spline. If not stated otherwise, energy is normalized so that $E = 0$ for $NH(x) + H$ with NH at equilibrium.

The contour plot of the $^4A''$ PES for the linear arrangement is shown in Fig. 3(a). The PES has an *early* transition state (TS),[23] i.e., the barrier is located in the entrance channel. After crossing the TS the reaction path steeply descends to the $N + H_2$ channel. The angle dependence of the PES for

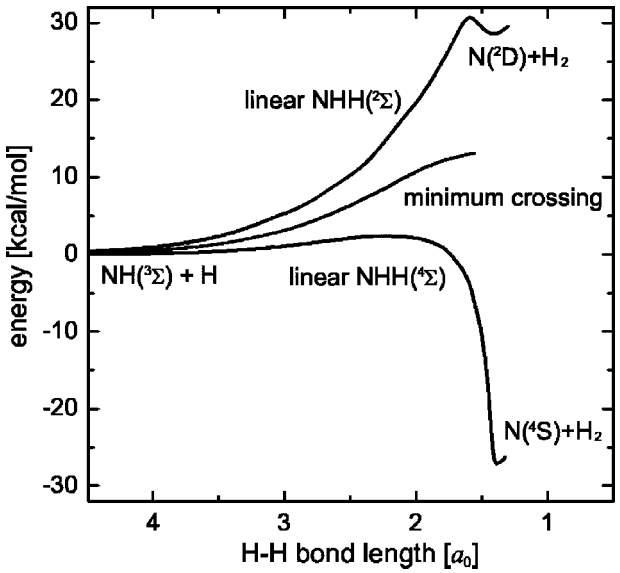

FIG. 4. Lower curve: Energy of the $^4A''$ PES along the minimum energy path in the linear arrangement. Upper curve: Energy of the $^2A''$ PES in the linear N–H–H arrangement; the energy is minimized in the NH bond length. Middle curve: Energy at the crossing between the $^4A''$ and the $^2A''$ PESs, minimized with respect to both the bond angle α and the NH bond length.

fixed N–H bond distance is depicted in Fig. 3(b). It is clearly seen that for low collision energies the reaction can only occur near the linear approach. The global PES calculated in this study is very similar to the one constructed by Pascual *et al.*;[11] however, our PES is much smoother. The potential energy along the minimum energy path of the $^4A''$ PES is shown in Fig. 4.

B. Trajectory calculations

Cross sections $\sigma(E_c,\nu,j)$ for reaction (1a) are calculated by classical trajectories as functions of the collision energy E_c and the initial vibrational ($\nu=0$, 1, and 2) and rotational (j) states of NH($X\,^3\Sigma$).[24] The collision energy is varied up to 140 kcal/mol and $0\leqslant j\leqslant 20$. The internal energy of NH(X) is initially set to the quantum mechanical zero-point energy for a particular state (ν,j). The maximum impact parameter is separately adjusted for each collision energy. For each E_c,j, and ν, 10 000 trajectories are calculated.

The results of the cross section calculations are depicted in Fig. 5. Because of the barrier in the entrance channel the cross sections steeply rise with E_c before they reach a plateau at around 20 kcal/mol. For $j=0$ the threshold occurs around $E_c\approx 0.5$ kcal/mol and then gradually shifts to higher energies with increasing j [Fig. 5(a)]. This shift is the result of the narrow transition state; faster and faster rotation of NH($X\,^3\Sigma$) makes the crossing of the TS region less and less probable. A similar effect has been observed for the $O+O_2$ reaction.[25] For reaction (1a) this trend is reversed between $j=10$ and 15, when the threshold starts to shift back to smaller energies. At higher collision energies [Fig. 5(b)] the cross section shows a more regular behavior with j; it simply increases with increasing j. The cross sections calculated in this work are very similar to those determined by Pascual *et al.*[11]

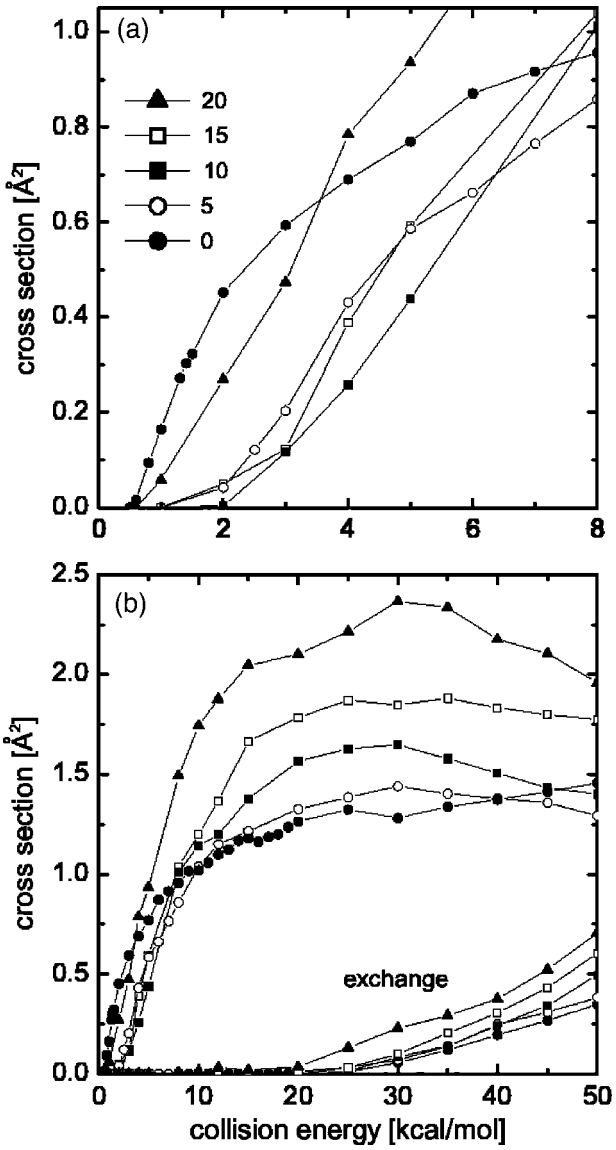

FIG. 5. (a) Reaction cross sections $\sigma(E_c,\nu,j)$ for reaction (1a) as function of the collision energy for $\nu=0$ and selected values of j. (b) The same as in (a), but for a larger energy range. The cross sections labeled by "exchange" are for the exchange reaction $NH(^3\Sigma)+H'\rightarrow NH'(^3\Sigma)+H$.

The thresholds of the classical cross sections are all below the barrier energy of about 2.2 kcal/mol. This indicates that part of the zero-point energy of NH($X\,^3\Sigma$) is transferred to NH–H translational motion while H approaches NH. Because the N–H bond lengths for the free radical and for the TS are different, the coupling between the two stretching degrees of freedom is not zero in the region of the TS and therefore energy can flow from NH vibration to translation.

The H atom exchange reaction $NH(^3\Sigma)+H'\rightarrow NH'(^3\Sigma)+H$ is also possible on the $^4A''$ PES, but only at very high energies [$E_c>20$ kcal/mol, see Fig. 5(b)]. The TS for the H-atom exchange has an energy of 22.58 kcal/mol with respect to the H+HN asymptote (avqz basis set); the two H–N bond lengths are $2.361a_0$ and the H–N–H bond angle is 180°. Because of the high TS barrier this reaction is of no relevance at low temperatures. In any case, it would not make a contribution to the removal of NH(X).

The temperature dependent rate coefficient for reaction (1a) is calculated by

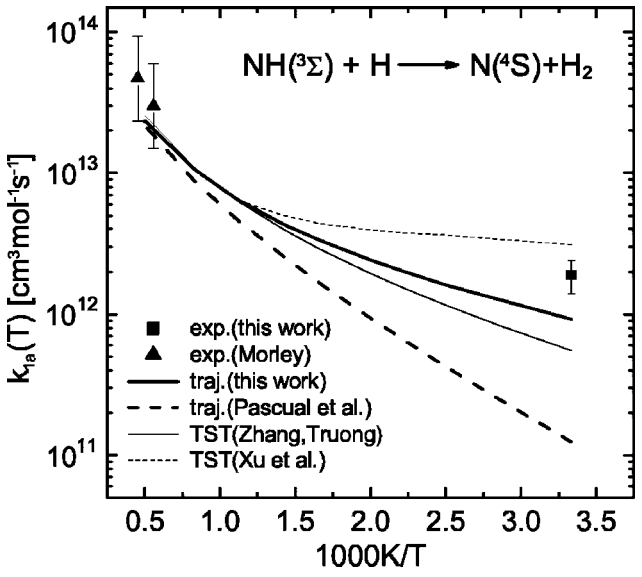

FIG. 6. Comparison of theoretical k_{1a} and experimental k_1 rate coefficients. The theoretical rates are taken from the trajectory (traj.) calculations of this work and of Pascual *et al.* (Ref. 11) and from the transition state theory (TST) calculations of Zhang and Truong (Ref. 10) and Xu *et al.* (Ref. 9).

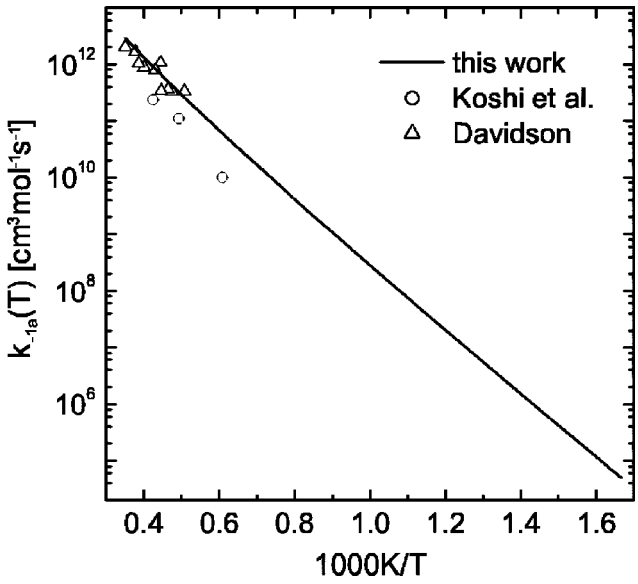

FIG. 7. Comparison of the calculated and measured rate coefficients k_{-1a} for the reaction $N(^4S)+H_2(X\,^1\Sigma_g^+)\rightarrow NH(X\,^3\Sigma^-)+H(^2S)$. ○ Koshi *et al.* (Ref. 5); △ Davidson and Hanson (Ref. 6).

$$k_{1a}(T)=\frac{\eta}{(\pi\mu)^{1/2}}\left(\frac{2}{k_BT}\right)^{3/2}Q^{-1}\sum_{\nu}\sum_{j}(2j+1)\times\exp(-E_{\nu j}/k_BT)\times\int_0^{\infty}E_c\sigma(E_c,\nu,j)\exp(-E_c/k_BT)dE_c, \quad (5)$$

where μ is the reduced mass of NH+H, k_B is Boltzmann's constant, Q is the vibrational-rotational partition function, and $E_{\nu j}$ is the energy of NH(X) in state (ν,j). The electronic degeneracy factor η is taken as $2/3$ because the quartet state $^4A''$ and the doublet (ground) state $^2A''$ both correlate with $NH(X\,^3\Sigma)+H(^2S)$ (Fig. 1).

The rate coefficient k_{1a} is calculated for a temperature range $300\ \mathrm{K}\leqslant T\leqslant 2000\ \mathrm{K}$; the value for $T=300$ K is $k_{1a}=0.92\times10^{12}$ cm^3 mol^{-1} s^{-1}. For the entire temperature range the rate coefficient can be represented by

$$k_{1a}(T)=1.88\times10^{8}T^{1.55}\exp(-103.2/T) \quad (6)$$

with T given in K and k_{1a} has units of cm^3 mol^{-1} s^{-1}. The calculated rate coefficient k_{1a} is compared with the experimental rate coefficient $k_{1a}(T=300\ \mathrm{K})$ and the three previous theoretical rates in Fig. 6.

IV. DISCUSSION

Our measurement of the rate coefficient for reaction (1a) k_{1a} is the first direct measurement at room temperature. The significant scatter of the experimental values explains the relatively large uncertainty and reflects the experimental difficulties. The two values of Morley[3] at temperatures around $T=2000$ K are more than an order of magnitude larger. The strong temperature dependence hints towards a sizable reaction barrier and the existence of a reaction threshold.

The possible products of reaction (1) are $NH_2(\tilde{X})$ (after stabilization in the $\tilde{X}\,^2A''$ ground state) and $N(^4S)+H_2(X\,^1\Sigma)$. Within the experimental uncertainty the measured rate coefficients are independent of the overall pressure, indicating that the stabilization of NH_2 by collisions with bath gases is unimportant at these low pressures. The $N(^4S)+H_2(X\,^1\Sigma)$ product channel can be accessed by a direct reaction on the $^4A''$ PES or by a spin-forbidden transition from state $^2A''$ to state $^4A''$ followed by an exchange reaction. The latter pathway is unlikely because, first, spin-orbit transitions for light atoms are generally weak and, second, the energy at the crossing of the two PESs is an increasing function of the H–H bond (Fig. 4).[26] Thus, in terms of energy, hopping from the $^2A''$ PES to the $^4A''$ PES is possible only in the entrance channel. On the other hand, while the NH–H approach on the $^4A''$ PES is confined to near-linear geometries, the minimum energy path of the $^2A''$ PES occurs at bent geometries, that is, the $^2A''$ PES steeply rises when NH and H approach in the linear geometry (Fig. 4). In conclusion, the consumption of $NH(^3\Sigma)$ in collisions with $H(^2S)$ atoms is believed to exclusively proceed on the $^4A''$ PES.

The calculated rate coefficient for reaction (1a) at $T=300$ K is about a factor of 2 smaller than the experimental rate coefficient, slightly outside the experimental uncertainty. In view of the neglect of quantum effects (tunneling and conservation of zero-point energy) and some remaining uncertainty about the precise barrier height at the TS, the agreement within a factor of 2 is reasonable. Exact quantum mechanical reactive calculations will show to which extent this agreement is trustworthy. The calculated rates at high temperatures ($T=1790$ K and 2200 K) agree well (within the experimental uncertainty of a factor of 2) with the measured data of Morley:[3] 2.0 and 2.7×10^{13} cm^3 mol^{-1} s^{-1} compared to 3.0 and 4.7×10^{13} cm^3 mol^{-1} s^{-1}, respectively. The calculated rate coefficient shows a significantly stronger temperature dependence at temperatures above $T=570$ K than predicted from an Arrhenius behavior at low temperatures.

The rate coefficient calculated by Pascual *et al.*[11] around

room temperature [$k_{1a}(300\ \mathrm{K})=1.24\times10^{11}\ \mathrm{cm^3\ mol^{-1}\ s^{-1}}$] is considerably smaller than the value calculated in this study [$k_{1a}(300\ \mathrm{K})=9.2\times10^{11}\ \mathrm{cm^3\ mol^{-1}\ s^{-1}}$]. This deviation is surprising because the two PESs and the calculated reaction cross sections are quite similar. It may be explained by the very simple analytical expression used by Pascual *et al.*[11] to represent the reaction cross sections as functions of translational energy. The TST result of Zhang and Truong[10] is slightly smaller than our calculated rate coefficient; besides this, the temperature dependence is similar. The TST rate coefficient of Xu *et al.*[9] is higher than the rate calculated in this work. It shows a somewhat unusual temperature dependence; between $T=300$ K and 700 K the rate rises only very slightly with T. Of all the four theoretical studies, the level of electronic structure theory employed by Xu *et al.*[9] is the lowest. At high temperatures all calculated rate coefficients are very similar and agree similarly well with the results of Morley, which means that details of the PESs and the dynamics calculations become unimportant for higher collision energies.

Using the thermodynamical data[15] ΔH and ΔS for H, N, NH, and H_2 and the calculated rate coefficient for reaction (1a), we can evaluate the equilibrium coefficient K for the reactants and products of reaction (1a). With K and k_{1a} we then can calculate the rate coefficient for the backward reaction of reaction (1a), k_{-1a}, which has been measured at high temperatures.[5,6] The calculated k_{-1a} is compared in Fig. 7 with the experimental values. While the agreement with the data of Davidson and Hanson is excellent, the rate coefficients of Koshi *et al.*[5] are smaller by approximately a factor of 4. The reasonable agreement with both experimental sets of data underlines the consistency of the present trajectory calculations.

If instead of the reaction with H atoms the reaction

$$\mathrm{NH}(^3\Sigma)+\mathrm{D}(^2S)\rightarrow \text{products} \tag{7}$$

is considered, the isotope exchange reaction mainly proceeding on the $^2A''$ ground state PES, $NH(X)+D(^2S)\rightarrow NHD(\tilde{X})^{\ddagger}\rightarrow ND(X)+H(^2S)$, also contributes to the removal of NH(X). The rate coefficient for the latter reaction is expected to be much larger than that for the reaction occurring on the $^4A''$ PES and therefore dominates the removal of NH(X) radicals. The corresponding experiments and trajectory calculations are in progress.[27]

ACKNOWLEDGMENTS

The authors are grateful to Professor J. Troe for stimulating interest and financial support. Financial support from the Fonds der Chemischen Industrie is thankfully acknowledged.

[1] B. S. Haynes, Combust. Flame **28**, 81 (1977).
[2] B. S. Haynes, Combust. Flame **28**, 113 (1977).
[3] C. Morley, Symp. Int. Combust., The Combust. Inst. **18**, 23 (1981).
[4] V. Ya. Basevich and V. I. Vedeneev, Khim. Fiz. **7**, 1552 (1988).
[5] M. Koshi, M. Yoshimura, K. Fukuda, H. Matsui, K. Saito, M. Watanabe, A. Imamura, and C. Chen, J. Chem. Phys. **93**, 8703 (1990).
[6] D. F. Davidson and R. K. Hanson, Int. J. Chem. Kinet. **22**, 843 (1990).
[7] E. N. Aleksandrov, V. Ya. Basevich, and V. I. Vedeneev, Khim. Fiz. **13**, 90 (1994).
[8] C. Ottinger, M. Brozis, and A. Kowalski, Chem. Phys. Lett. **315**, 355 (1999).
[9] Z.-F. Xu, D.-C. Fang, and X.-Y. Fu, J. Phys. Chem. A **101**, 4432 (1997).
[10] S. Zhang and T. N. Truong, J. Chem. Phys. **113**, 6149 (2000).
[11] R. Z. Pascual, G. C. Schatz, G. Lendvay, and D. Troya, J. Phys. Chem. A **106**, 4125 (2002).
[12] T. Takayanagi, Y. Kurosaki, and K. Yokoyama, Chem. Phys. Lett. **321**, 106 (2000).
[13] W. Hack and A. Wilms, J. Phys. Chem. **93**, 3540 (1989).
[14] *CRC Handbook of Chemistry and Physics*, 83th ed., edited by D. R. Lede (CRC, Boca Raton, 2002).
[15] The thermodynamical data for ΔH (in kcal/mol) and ΔS [in cal/(mol K)] from Ref. 14 are 84.0/43.3 for NH; 52.1/27.4 for H; 112.9/36.6 for N; and 0.0/31.2 for H_2.
[16] H.-J. Werner and P. J. Knowles, J. Chem. Phys. **89**, 5803 (1988).
[17] P. J. Knowles and H.-J. Werner, Chem. Phys. Lett. **145**, 514 (1988).
[18] S. R. Langhoff and E. R. Davidson, Int. J. Quantum Chem. **8**, 61 (1974).
[19] H.-J. Werner and P. J. Knowles, J. Chem. Phys. **82**, 5053 (1985).
[20] P. J. Knowles and H.-J. Werner, Chem. Phys. Lett. **115**, 259 (1985).
[21] T. H. Dunning, Jr., J. Chem. Phys. **90**, 1007 (1989).
[22] H.-J. Werner, P. J. Knowles, R. Lindh *et al.*, MOLPRO, version 2002.6, a package of ab initio programs, 2003. See http://www.molpro.net
[23] R. D. Levine and R. B. Bernstein, *Molecular Reaction Dynamics and Chemical Reactivity* (Oxford University Press, Oxford, 1987).
[24] M. Karplus, R. N. Porter, and R. D. Sharma, J. Chem. Phys. **43**, 3259 (1965).
[25] P. Fleurat-Lessard, S. Yu. Grebenshchikov, R. Siebert, R. Schinke, and N. Halberstadt, J. Chem. Phys. **118**, 610 (2003).
[26] A global potential energy surface for the $^2A''$ state has been calculated on the same level of electronic structure theory as the potential for the $^4A''$ state. It will be published, together with trajectory calculations and the experiment for the exchange reaction $NH(X^3\Sigma^-)+D(^2S)\rightarrow ND(X^3\Sigma^-)+H(^2S)$, at a later date.
[27] Z.-W. Qu, H. Zhu, R. Schinke, L. Adam, and W. Hack J. Chem. Phys. (submitted).